

# Effects of Lateral Contact Stiffness and Geometrical Parameters on Torsional Sensitivity of Vibration Modes of Rectangular Atomic Force Microscopy Cantilevers with Sidewall

S. Bigham<sup>1</sup>, S. Yazdani<sup>1,\*</sup>, and J. Yazdani<sup>2</sup>

<sup>1</sup>School of Mechanical Engineering, University of Tehran, Tehran, Iran

<sup>2</sup>Nanoscience and Nanotechnology Research Center, Razi University, Kermanshah, Iran

Effects of sidewall and geometrical parameters and lateral contact stiffness on torsional sensitivity of vibration modes of rectangular AFM cantilevers are analyzed. When the normal contact stiffness ( $\beta_t$ ) increases the sensitivity of the first mode slowly decreases then rapidly decreases as the normal contact stiffness, increases approximately for  $\beta_t > 0.1$ . Results also indicate the first mode is more sensitive than other high-order modes. AFM without sidewall probe is more sensitive than the AFM with sidewall probe, especially and for high order modes. Results shows that AFM with higher sidewall length is more sensitive than AFM with lower sidewall length for  $\beta_t < 10$  and vice versa for  $\beta_t > 100$ . It is seen increasing the horizontal cantilever probe lengths increased the sensitivity. AFM with lower cross section width has lower torsional sensitivity. Also as cross section width of the cantilever probe thickness increases the torsional sensitivity decreases.

**Keywords:** Nanolithography, AFM, Vibration Response, Sidewall Scanning.

## 1. INTRODUCTION

In recent years, imaging and manipulating structures at the nanometer scale has been a subject for many researchers due to its various applications. Atomic force microscopy (AFM) systems are powerful and useful technique in nanoscale science and technologies such as surface science and biomaterials. AFM has been widely developed as an effective tool for obtaining atomic-scale images and the material surface properties.<sup>1–8</sup>

Some of these applications are nanolithography in MEMS (Micro Electro-Mechanical Systems) and NEMS (Nano Electro-Mechanical Systems)<sup>9–11</sup> and surface characterization in material science, to the study of living biological systems in their natural environment, to nanolithography and topographical analysis of soft materials such as DNA and lubricant molecules.

In AFM systems, a sharp probe at the end of a cantilever interacting locally with the sample surface is scanned by a piezoelectric scanner, providing three-dimensional information about the surface. It is well known that a customary cantilever with a tip at the free end plays an important role

in AFM measurements. When a tip scans across a sample surface, it induces a dynamic interaction force between the tip and the surface.

Dynamic responses of the AFM cantilever have been investigated by many researches.<sup>12–18</sup> Some of researchers<sup>19–24</sup> have been studied the vibration response of an AFM cantilever for convenience without considering the interactive damping Turner et al.<sup>25</sup> and Rabe et al.,<sup>26</sup> have been shown the effect of damping on the vibration response of an AFM cantilever is very important.

Effect of interactive damping on sensitivity of vibration modes of rectangular AFM cantilevers have been investigated by Chang et al.<sup>27</sup> Long Lee and Chang<sup>28</sup> have been studied Coupled lateral bending and torsional vibration sensitivity of atomic force microscope cantilever. More recently Yazdani et al.<sup>29</sup> have been presented the analytical solution of interactive damping and longitudinal and normal contact stiffness on sensitivity of vibration modes of rectangular AFM cantilevers. Mahdavi et al.<sup>30</sup> presented a more comprehensive modeling of atomic force microscope cantilever. They used Timoshenko beam theory in their analysis. Chang et al.<sup>31</sup> studied the sensitivity of the first four flexural modes of an AFM cantilever with a sidewall probe. Their results showed that a sidewall scanning AFM

\* Author to whom correspondence should be addressed.

is more sensitive when the contact stiffness is lower and that the first mode is the most sensitive. Also they found the resonance frequency of an AFM cantilever is low when contact stiffness is small, however, the frequency rapidly increases as contact stiffness increases.

The objective of the current study is to investigate sensitivity of the torsional modes of an AFM cantilever with a sidewall probe and study effect of sidewall and other geometrical parameters on the torsional modal sensitivity.

## 2. ANALYSIS

Figure 1 shows the schematic of an AFM with sidewall with uniform cross section thickness  $a$ , width  $b$ , length  $L$  for horizontal cantilever and  $h$  for vertical extension. An AFM probe is suitable for sidewall scanning. An AFM with sidewall consists of a horizontal cantilever and a vertical extension at the free end, and a tip located at the free end of the vertical extension is able to probe in a direction perpendicular to sidewall. The probe named as ‘‘Assembled Cantilever Probe.’’<sup>31</sup> In the analysis, the horizontal cantilevers and vertical extension are considered as an elastic beam. The cantilever experiences torsional vibrations during contact with the sample. When the AFM cantilever tip interacts with the sample by a lateral spring  $K_t$ , the cantilever will vibrate torsional.

The linear differential equation of motion for the torsional vibration of the cantilever can be expressed as<sup>32</sup>

$$G\eta \frac{\partial^2 \theta(x, t)}{\partial x^2} = \rho I_p \frac{\partial^2 \theta(x, t)}{\partial t^2} \quad (1)$$

where  $\theta$  is the angle of torsion of the cross-sectional area,  $G$  is the modulus of shear,  $I_p$  is the polar moment of area,  $\eta$  is the torsional parameter for a rectangular bar and is given by<sup>33</sup>

$$\eta = \frac{1}{3} ab^3 \left( 1 - 0.63 \frac{a}{b} \right) \quad (2)$$

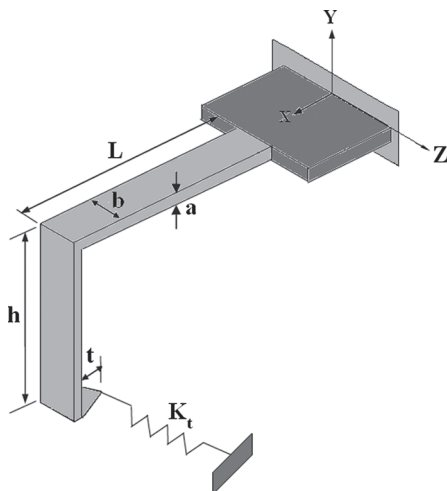


**Fig. 1.** Schematic diagram of an AFM cantilever micro assembled with a vertical extension at the free end and a tip located at the free end of the vertical extension.

The boundary conditions are

$$\theta(0, t) = 0 \quad (3)$$

$$G\eta \frac{\partial \theta(L, t)}{\partial x} = -K_t h^2 \theta(L, t) - J_0 \frac{\partial^2 \theta(L, t)}{\partial t^2} \quad (4)$$

where  $J_0$  is moment of inertia of the vertical extension. Equation (3) is the condition of the cantilever beam end being fixed, and Eq. (4) is the force balance at  $x = L$  with the linear spring constant  $K_t$ , depending on the interaction between the tip and sample and moment of inertia of the vertical extension.

A general solution of Eq. (1), with boundary condition (3) and (4) can be expressed as

$$\theta(x, t) = \psi(x) \exp(i\omega t) \quad (5)$$

where  $\omega$  is the angular frequency. Substituting Eq. (5) into Eq. (1)

$$\psi(x) = A \sin \left( \sqrt{\frac{\rho I_p}{G\eta}} x \right) + B \cos \left( \sqrt{\frac{\rho I_p}{G\eta}} x \right) \quad (6)$$

where  $A$  and  $B$ , are constants determined from the boundary conditions. Substituting Eq. (6) into Eq. (3) yield  $B = 0$ . Substituting Eq. (6) into Eq. (4) the characteristics equation can be found:

$$Ch(\gamma, \beta_t) = \gamma \cos(\gamma) + \left( \beta_t - J_0 \frac{\gamma^2}{\rho L I_p} \right) \sin(\gamma) = 0 \quad (7)$$

where  $\gamma = \sqrt{(\rho I_p)/(G\eta)} L \omega$  and  $\beta_t = (Lh^2)/(G\eta)K_t$  is the normal stiffness ratio between the torsional contact stiffness and that of the cantilever. The relationship between frequency and  $\gamma$  is given by

$$f = \frac{1}{2\pi L} \sqrt{\frac{G\eta}{\rho I_p}} \gamma \quad (8)$$

The relationship between torsional frequency  $f_t$  and contact stiffness  $\beta_t$  can be expressed as

$$\frac{\partial f_t}{\partial \beta_t} = \frac{\partial f_t}{\partial \gamma} \frac{\partial \gamma}{\partial \beta_t} \quad (9)$$

The torsional sensitivity of the cantilever can be calculated from the frequency, which can be measured. The sensitivity of the mode of the cantilever changes significantly for small variations of stiffness as the cantilever crosses the sample. Differentiation of Eq. (7) with respect to  $\beta_t$

$$\frac{d\gamma}{d\beta_t} = - \frac{\partial Ch/\partial \beta_t}{\partial Ch/\partial \gamma} \quad (10)$$

Form Eqs. (7), (9) and (10) the following equation is obtained

$$\frac{\partial f}{\partial \beta_t} = - \frac{1}{2\pi L} \sqrt{\frac{G\eta}{\rho I_p}} \times \frac{\sin(\gamma)}{(\beta_t - J_0/(\rho L I_p) + 1) \cos(\gamma) - (1 + 2J_0/(\rho L I_p)) \gamma \sin(\gamma)} \quad (11)$$

Equation (11) can be expressed in normalized form as

$$S_t = \frac{df/d\beta_n}{1/(2\pi L)\sqrt{G\eta/\rho I_p}} \quad (12)$$

From Eq. (12) dimensionless torsional sensitivities for each vibration mode of an AFM cantilever with a sidewall can be calculated.

### 3. RESULTS AND DISCUSSION

The torsional sensitivity of the vibration modes of an AFM cantilever with a sidewall probe has been investigated. In order to know the effect of relative parameters on the sensitivity and resonant frequency, the following geometric and material parameters are considered:  $G = 66.4$  (G Pa),  $\rho = 2330$  kg/m<sup>3</sup>,  $L = 300$  mm,  $a = 2$  μm,  $b = 50$  μm,  $h = 150$  μm. Figure 2 shows effects of lateral contact stiffness of an AFM cantilever without a sidewall probe on the normalized torsional modal sensitivities for the first six modes. Results have excellent agreement with reference.<sup>27</sup>

It can be seen the torsional sensitivities of the first mode for lower lateral contact stiffness has maximum sensitivity and is constant approximately for  $\beta_t < 0.1$  and then  $S_t$  is fallen. For the higher modes (modes 2–6), torsional sensitivities is fallen slower and later than first mode. Figure 3 represents the variation of the normalized torsional modal sensitivities of the first mode with respect to lateral lateral contact stiffness of an AFM cantilever with a sidewall probe. It can be seen that, the sensitivity of the first mode slowly decreases as the normal contact stiffness ( $\beta_t$ ) increases then rapidly decreases as the normal contact stiffness, increases at  $\beta_t > 0.1$ .

Also it is found that the maximum value for the sensitivity of the first mode is 0.1142. The variation of the

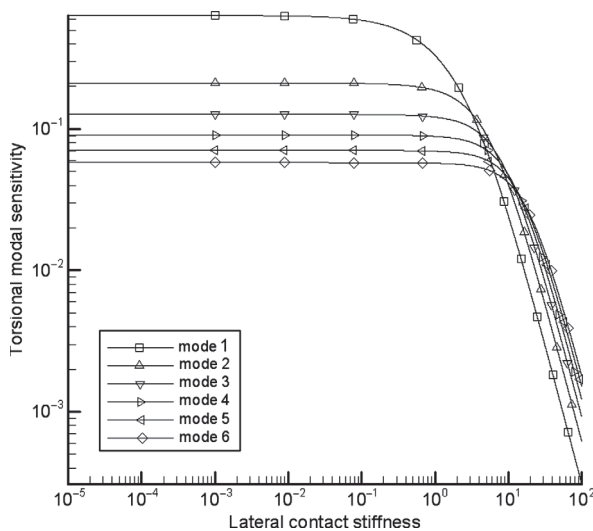


**Fig. 2.** The effect of lateral contact stiffness on the normalized torsional modal sensitivity for an AFM cantilever without a sidewall probe.

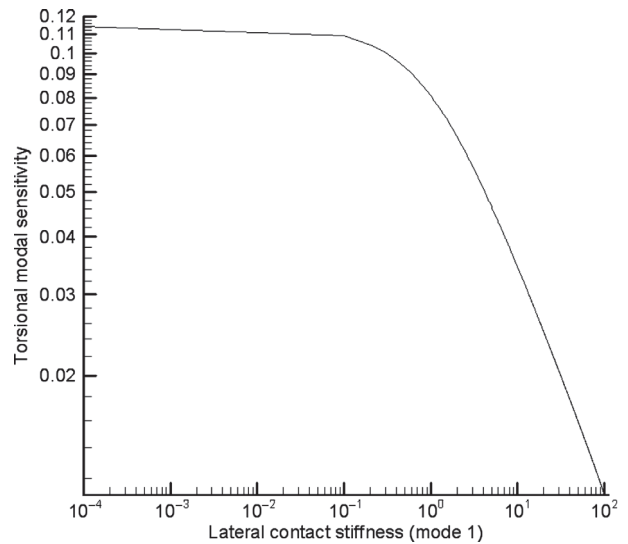


**Fig. 3.** The effect of lateral contact stiffness on the normalized torsional modal sensitivity for an AFM cantilever with a sidewall probe, (mode 1).

normalized torsional modal sensitivities with respect to lateral contact stiffness of an AFM cantilever with a sidewall probe is illustrated in Figure 4, for the high order modes (modes 2–6). It is found that the effect of lateral contact stiffness on the normalized torsional modal sensitivity of modes (2–6) is quite deference with regards to the first mode. Comparing Figures 3 and 4 it can be inferred

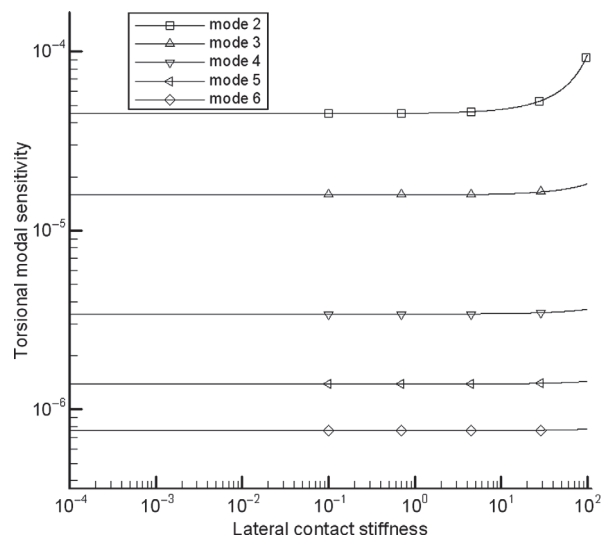
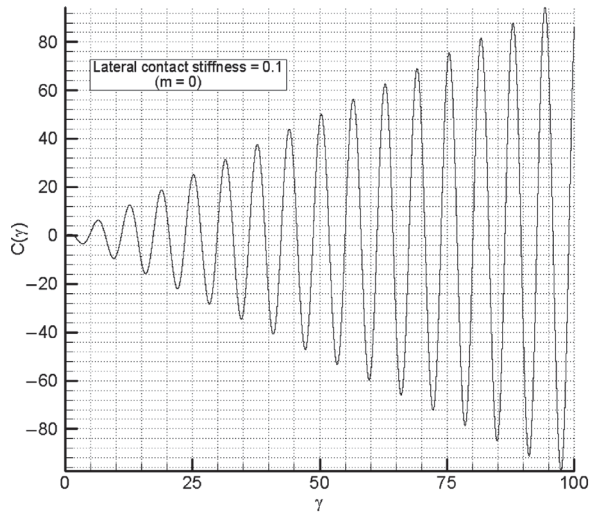


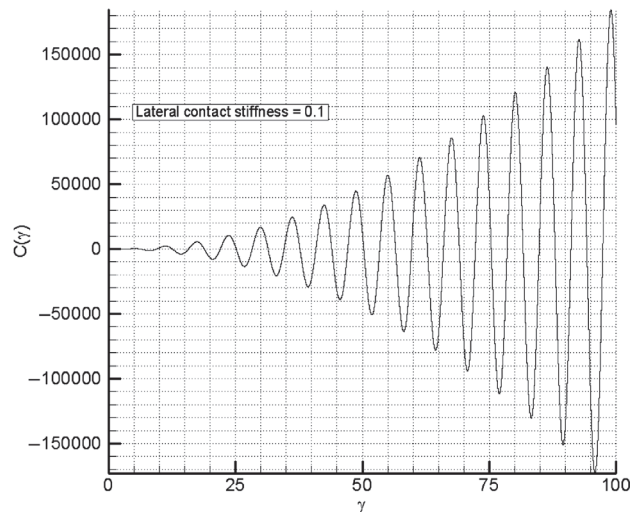
**Fig. 4.** The effect of lateral contact stiffness on the normalized torsional modal sensitivity for an AFM cantilever with a sidewall probe, (modes 2–6).

**Table I.** The minimum values of torsional modal sensitivity.

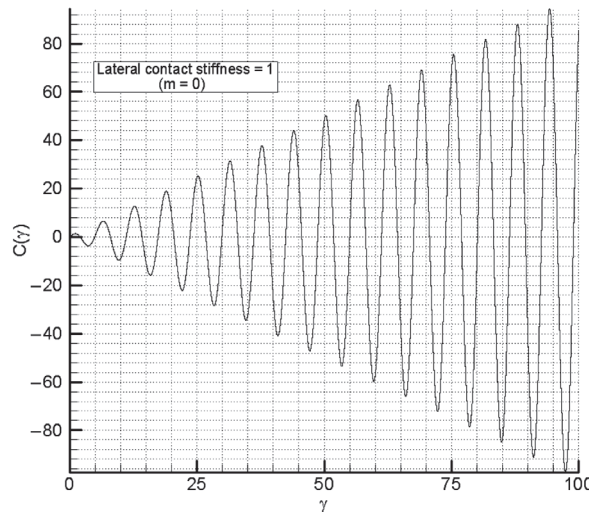
Mode 2	Mode 3	Mode 4	Mode 5	Mode 6
$4.498 \times 10^{-5}$	$1.5792 \times 10^{-5}$	$3.4437 \times 10^{-6}$	$1.3872 \times 10^{-6}$	$7.6060 \times 10^{-7}$



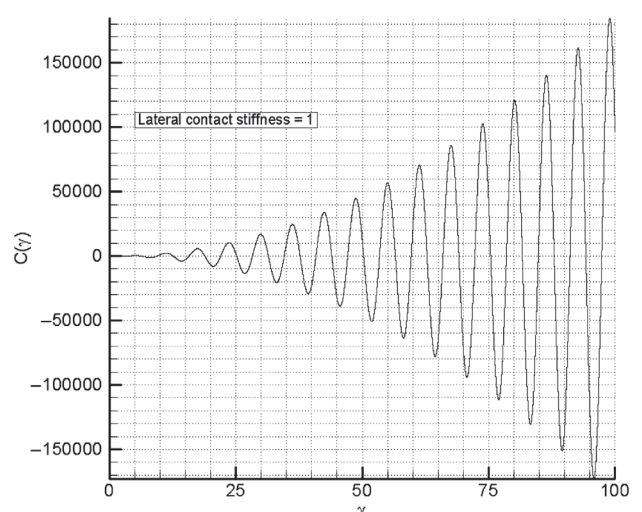
(a)



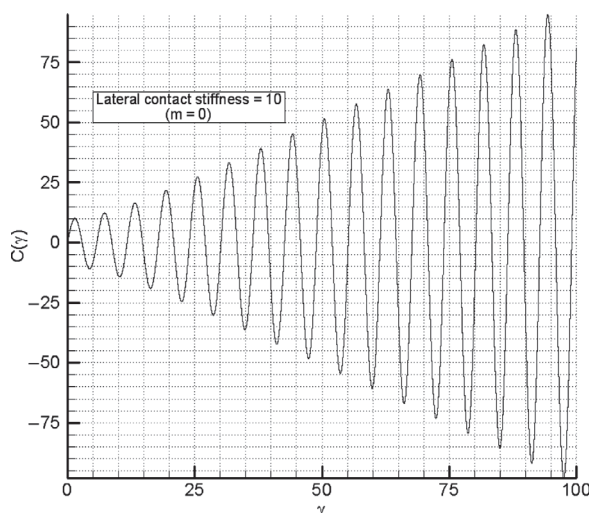
(d)



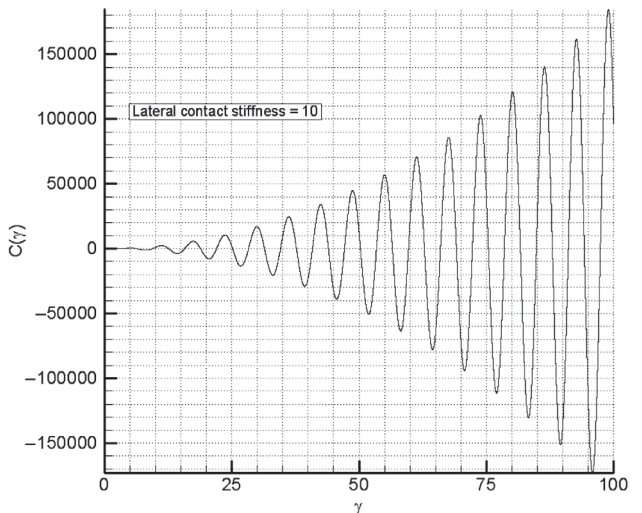
(b)



(e)



(c)



(f)

Fig. 5. Diagram of eigenvalues: (a) to (c) AFM without sidewall, (d) to (f) AFM with sidewall.

that the first mode is more sensitive than other high-order modes, (modes 2–6). For  $\beta_t < 10$  the normalized torsional modal sensitivity is approximately constant and then sensitivity increased slowly as  $\beta_t$  increased for the second mode and the variation of normalized torsional modal sensitivity with respect to lateral contact stiffness for mode 3 to mode 6 is very inconspicuous. With Comparing Figures 2, 3 and 4 it can be found the sidewall probe is very effective on the normalized torsional modal sensitivity. Also AFM without sidewall probe is more sensitive than the AFM with sidewall probe and it is more sensible for high order modes.

The minimum values of torsional modal sensitivity for mode 2 to mode 6 are listed in Table I.

Diagram of the  $C(\gamma)$  with respect to  $\gamma$  is shown in Figures 5(a–c) for an AFM without sidewall and Figures 5(d–f) for an AFM with side wall for  $\beta_t = 10^{-1}$ ,  $10^0$  and  $10^1$  where  $C(\gamma)$  is defined by follow equation

$$C(\gamma) = \gamma \cos(\gamma) + \left( \beta_t - J_0 \frac{\gamma^2}{\rho L I_p} \right) \sin(\gamma) \quad (13)$$

The eigenvalues are roots of  $C(\gamma)$ . It can be seen diagram is similar to stretches spring for the AFM with sidewall with respect to AFM without side wall.

In order to better design of an AFM effects of geometrical parameter on the normalized torsional modal sensitivities are investigated. Figure 6 indicates effect of sidewall length on the normalized torsional modal sensitivities of mode 1. For  $\beta_t < 10$ , AFM with higher sidewall length is more sensitive and for  $\beta_t > 100$ , AFM with higher sidewall length has lower torsional sensitivity.

As lateral contact stiffness increases the AFM with sidewall has lower torsional modal sensitivities for lower sidewall length. Maximum values of first mode for

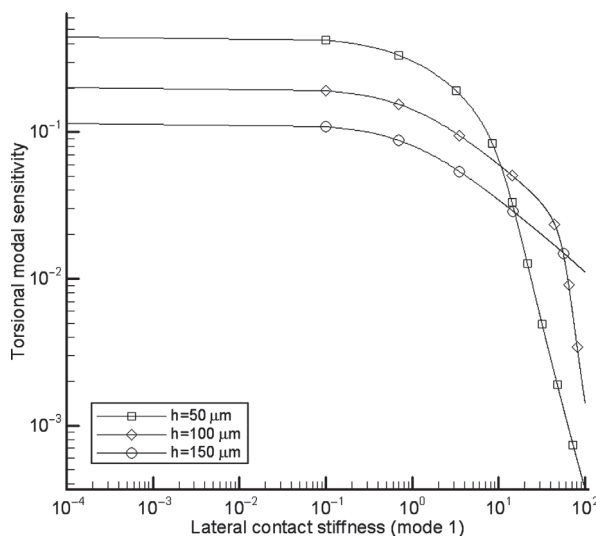


**Fig. 6.** Normalized torsional sensitivity of mode 1 versus lateral contact stiffness for an AFM cantilever at various tip lengths.

**Table II.** Max value of first mode at  $L = 300 \mu\text{m}$ ,  $b = 50 \mu\text{m}$  and  $a = 2 \mu\text{m}$ .

$h = 50 \mu\text{m}$	$h = 100 \mu\text{m}$	$h = 150 \mu\text{m}$
0.4439	0.2014	0.1142

various values of sidewall length are shown listed in Table II.

Figure 7 indicates Normalized torsional sensitivity of mode 1 as function of the lateral contact stiffness for an AFM cantilever at various horizontal cantilever probe lengths. It is seen increasing the horizontal cantilever probe lengths increased the sensitivity.

Maximum values of first mode for various values of sidewall length are listed in Table III.

Normalized torsional sensitivity of mode 1 as function of the lateral contact stiffness for an AFM cantilever at various cross section widths of the cantilever probe lengths is shown in Figure 8. AFM with lower cross section width has lower torsional sensitivity.

Table IV contains the maximum values of first mode for various values of cross section widths.

Figure 9 represents the variation of the normalized torsional sensitivity of mode 1 with respect to lateral contact stiffness for an AFM cantilever at various cross section thickness of the cantilever probe thickness. It is seen as cross section width of the cantilever probe thickness increases the torsional sensitivity decreases.

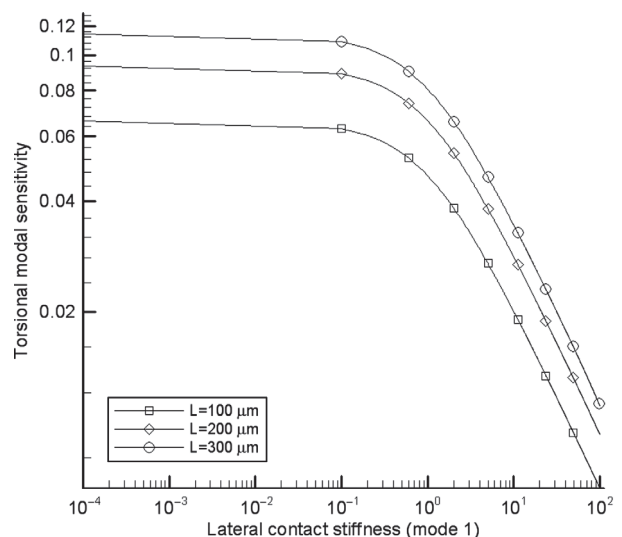


**Fig. 7.** Normalized torsional sensitivity of mode 1 versus lateral contact stiffness for an AFM cantilever at various horizontal cantilever probe lengths.

**Table III.** Max value of first mode at  $h = 150 \mu\text{m}$ ,  $b = 50 \mu\text{m}$  and  $a = 2 \mu\text{m}$ .

$L = 100 \mu\text{m}$	$L = 200 \mu\text{m}$	$L = 300 \mu\text{m}$
$6.6329 \times 10^{-2}$	$9.3522 \times 10^{-2}$	0.1142

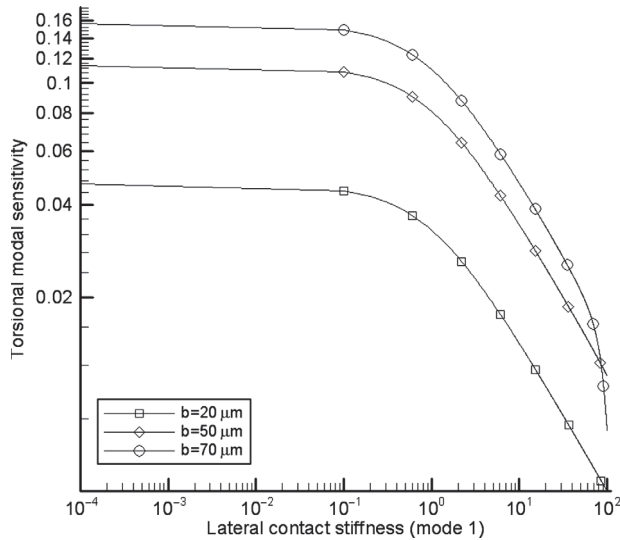


**Fig. 8.** Normalized torsional sensitivity of mode 1 versus lateral contact stiffness for an AFM cantilever at various cross section widths of the cantilever probe lengths.

**Table IV.** Max value of first mode at  $L = 300 \mu\text{m}$ ,  $h = 150 \mu\text{m}$  and  $a = 2 \mu\text{m}$ .

$b = 20 \mu\text{m}$	$b = 50 \mu\text{m}$	$b = 70 \mu\text{m}$
$4.6759 \times 10^{-2}$	0.1142	0.1566

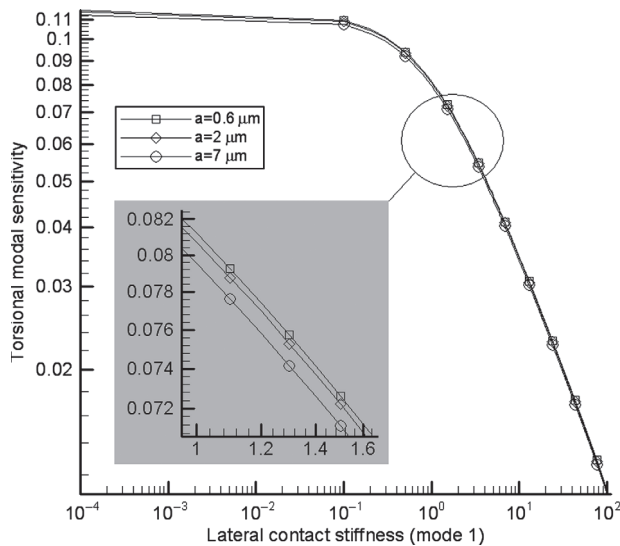


**Fig. 9.** Normalized torsional sensitivity of mode 1 as function of the lateral contact stiffness for an AFM cantilever at various cross section thicknesses of the cantilever probe lengths.

**Table V.** Max value of first mode at  $L = 300 \mu\text{m}$ ,  $h = 150 \mu\text{m}$  and  $b = 50 \mu\text{m}$ .

$a = 0.6 \mu\text{m}$	$a = 2 \mu\text{m}$	$a = 7 \mu\text{m}$
0.1149	0.1142	0.1125

Maximum values of values of first mode for various values of cross section width of the cantilever probe thickness are listed in Table V.

## 4. CONCLUSION

The torsional sensitivity of the vibration modes of an AFM with sidewall has been investigated. According to the analysis, the sensitivity of the first mode slowly decreases as the normal contact stiffness ( $\beta_i$ ), increases then rapidly decreases as the normal contact stiffness, increases approximately at  $\beta_i > 0.1$ . Results also indicate, the first mode is more sensitive than high-order modes (modes 2–6). Results showed sidewall probe is very effective on the normalized torsional modal sensitivity. Also AFM without sidewall probe is more sensitive than the AFM with sidewall probe. Also effects of geometrical parameters for an AFM cantilever with a sidewall probe have been investigated. Results shows that AFM with higher sidewall length is more sensitive than AFM with lower sidewall length for  $\beta t < 10$  and vice versa for  $\beta t > 100$ . It was seen increasing the horizontal cantilever probe lengths increased the sensitivity. AFM with lower cross section width has lower torsional sensitivity. Also as cross section width of the cantilever probe thickness increases the torsional sensitivity decreases.

## References

1. K. Holmberg and A. Matthews, *Coatings Tribology: Properties, Techniques and Applications in Surface Engineering*, Elsevier, New York (1994).
2. P. E. Mazeran and J. L. Loubet, *Tribol. Lett.* 7, 199 (1999).
3. B. Bhushan, *Handbook of Micro/Nanotribology*, 2nd edn., CRC, Boca Raton, FL (1999).
4. F. J. Giessibl, *Advances in Atomic Force Microscopy, Reviews of Modern Physics* 75, 949 (2003).
5. R. Garcia and R. Perez, *Surface Science Report* 47, 197 (2002).
6. S. Lin, J. L. Chen, L. S. Huang, and H. W. Lin, *J. Curr. Proteomics* 2, 55 (2005).
7. R. J. Colton, *J. Vac. Sci. Technol. B* 22, 1609 (2004).
8. N. Jalili and K. Laxminarayana, *J. Mechatron.* 14, 907 (2004).
9. T. H. Fang and W. J. Chang, *J. Phys. Chem. Solids* 64, 913 (2003).
10. W. J. Chang, T. H. Fang, and C. I. Weng, *Nanotechnology* 15, 427 (2004).
11. T. H. Fang, W. J. Chang, and C. I. Weng, *Mater. Sci. Eng. A* 430, 332 (2006).
12. O. Nakabeppu, M. Chandrachood, Y. Wu, J. Lai, and A. Majumdar, *Appl. Phys. Lett.* 66, 694 (1995).
13. U. Rabe, K. Janser, and W. Arnold, *Rev. Sci. Instrum.* 67, 3281 (1996).
14. T. Drobek, R. W. Stark, M. Graber, and W. M. Heckl, *New J. Phys.* 1, 151 (1999).
15. M. Ashhab, M. V. Salapaka, M. Dahleh, and I. Mezić, *Automatica* 35, 1663 (1999).
16. O. B. Wright and N. Nishiguchi, *Appl. Phys. Lett.* 71, 626 (1997).
17. P. E. Mazeran and J. L. Loubet, *Tribology Lett.* 7, 199 (1999).
18. W. Weaver, Jr., S. P. Timoshenko, and D. H. Young, *Vibration Problems in Engineering*, 5th edn., Wiley, New York (1990).
19. S. Hirsekorn, U. Rabe, and W. Arnold, *Nanotechnology* 8, 57 (1997).

20. K. Yamanaka, A. Noguchi, T. Tsuji, T. Koike, and T. Goto, *Surf. Interface Anal.* 27, 600 (1999).
21. G. G. Yaralioglu, F. L. Degertekin, K. B. Crozier, and C. F. Quate, *J. Appl. Phys.* 87, 7491 (2000).
22. R. F. Fung and S. C. Huang, *ASME J. Vibr. Acoust.* 123, 502 (2001).
23. R. Levy and M. Maaloum, *Nanotechnology* 13, 33 (2002).
24. H. Kawakatsu, S. Kawai, D. Saya, M. Nagashio, D. Kobayashi, and H. Toshiyoshi, *Rev. Sci. Instrum.* 73, 2317 (2002).
25. J. A. Turner, S. Hirsekorn, U. Rabe, and W. Arnold, *J. Appl. Phys.* 82, 967 (1997).
26. U. Rabe, J. A. Turner, and W. Arnold, *Appl. Phys. A* 66, S277 (1998).
27. W.-J. Chang, T.-H. Fang, and H.-M. Chou, *Phys. Lett. A* 312, 158 (2003).
28. H.-L. Lee and W.-J. Chang, *Ultramicroscopy* 108, 707 (2008).
29. J. Yazdani, S. Yazdani, and S. Bigham, *Digest Journal of Nanomaterials and Biostructures* 3, 277 (2008).
30. M. H. Mahdavi, A. Farshidianfar, M. Tahani, S. Mahdavi, and H. Dalir, *Ultramicroscopy* 109, 54 (2008).
31. W.-J. Chang, H.-L. Lee, and T. Y.-F. Chen, *Ultramicroscopy* 108, 619 (2008).
32. W. J. Weaver, S. P. Timoshenko, and D. H. Young, *Vibration Problems in Engineering*, 5th edn., Wiley, New York (1990).
33. S. Timoshenko and J. N. Goodier, *Theory of Elasticity*, McGraw-Hill, New York (1987).

Received: 21 January 2009. Accepted: 3 April 2009.